Numerical simulation of magnetic-flux penetration in concentric circular arrays of Josephson junctions

C. Auletta
Dipartimento di Informatica, Università degli Studi di Salerno, 84081 Baronissi (SA), Italy

R. De Luca and S. Pace
Dipartimento di Fisica, Università degli Studi di Salerno, 84081 Baronissi (SA), Italy

G. Raiconi
Dipartimento di Informatica, Università degli Studi di Salerno, 84081 Baronissi (SA), Italy
(Received 9 November 1992; revised manuscript received 5 February 1993)

We present a numerical analysis of the stationary magnetic states realized in a planar system of concentric circular arrays of Josephson junctions coupled through identical inductances. In particular, a magnetization experiment is simulated by analyzing the flux distribution upon application of an external magnetic field in the direction orthogonal to the system after zero-field cooling. It is shown that this system can be adopted as a Josephson-junction-array model of sintered high-T_c superconductors.

I. INTRODUCTION

The diamagnetic response of a superconducting ring interrupted by a Josephson junction (JJ) has been extensively studied in the past.[1,2] In these systems the stationary magnetic states are obtained by minimizing the potential $G[\Phi]$ with respect to the flux Φ linked to the ring. This potential consists of two terms: The first term is the energy of an isolated Josephson junction G_J, expressed as follows:

$$G_J=[I_J(h,T)\Phi_0/2\pi][1-\cos(2\pi\Phi/\Phi_0)] ,$$

where I_J is the field- and temperature-dependent maximum Josephson current and Φ_0 is the elementary flux quantum; the second term, G_m, is the energy of the circulating current I_S, which is given by $G_m=LI_S^2/2=(\Phi-\Phi_{\rm ext})^2/2L$, where $\Phi_{\rm ext}$ is the geometrical flux due to the applied magnetic field H; i.e., $\Phi_{\rm ext}=\mu_0 HS$, μ_0 and S being the permeability of vacuum and the geometrical area of the ring, respectively. In order to check the validity of the above expressions one has to recall that the current I in the Josephson element and the voltage V across it are linked, respectively, to the gauge-invariant superconducting phase difference φ across the JJ and to its time derivative, according to the Josephson constitutive equations:[3]

$$I=I_J\sin\varphi , \tag{1a}$$

$$V=(\Phi_0/2\pi)d\varphi/dt . \tag{1b}$$

In addition, fluxoid quantization imposes that the superconducting phase φ be linked to the flux Φ through the following relation:[3]

$$\varphi+2\pi\Phi/\Phi_0=2\pi n , \tag{2}$$

where n is an integer, which under zero-field cooling (ZFC) conditions is equal to zero. Now, any stationary current $I_S=(\Phi-\Phi_{\rm ext})/L$ circulating in the JJ must equal the derivative of G_J with respect to Φ; i.e., any stationary magnetic state must lie in a relative minimum of the Gibbs potential G. Therefore, by using our expression of G and setting $\delta G/\delta\Phi=0$, we obtain the same expression as in Eq. 1(a) in which one takes $I=I_S$, and, according to Eq. 2, $\varphi=-2\pi\Phi/\Phi_0+2\pi n$.

In this paper we generalize the analysis of a single superconducting ring containing a single JJ to a set of concentric superconducting rings, each one containing a number n_k (where k is the index referring to the kth ring) of identical junctions. The number of junctions n_k is taken to be directly proportional to the perimeter of the kth ring. A schematic representation of this system is given in Fig. 6, where we take the inductance of the kth ring L_k proportional to the normal area S_k enclosed. In the first part of this work we show that this particular network of Josephson junctions and inductances can be adopted to describe the low-field diamagnetic response of Josephson-junction arrays viewed as models of granular superconductors.[4] Majhofer, Wolf, and Dieterich[5] and Dominguez and José[6] have already investigated the electrodynamical properties of two-dimensional (2D) overdamped Josephson-junction square arrays taking into account the screening current effects by inductively coupling the Josephson junctions of the network. The concentric ring model, though being simpler than the one adopted by the aforementioned authors, can be shown to capture the essential features of the diamagnetic response of granular superconductors. For this model, then, we study the process of flux penetration upon application of an external magnetic field in the direction orthogonal to the network of JJ's and inductances, after cooling the system down to temperatures lower than the critical temperature of the superconducting material in the absence of magnetic field; i.e., after ZFC. We follow the evolution of the system to its stationary solution at very low tem-

peratures, so that thermally activated flux penetration can be neglected, and record the field and current distribution in the system at equilibrium for cyclically varying values of the external field. In this way we are able to draw hysteresis cycles for the magnetic variables involved in the problem resulting from the irreversible character of the flux penetration mechanism.

II. THE ASYMMETRIC MODEL

In this section we shall show that the low-field diamagnetic properties of granular superconductors can be described by means of a model consisting of a set of concentric superconducting rings containing inductively coupled identical Josephson junctions.

A. The equations

We start our analysis by studying the process of flux penetration in a simple system consisting of three concentric granular shells, each shell containing N grains. The weak superconducting coupling between adjacent grains is described by Josephson junctions, and the magnetic screening effects are taken into account by coupling these junctions through inductances. The coupling Josephson energy[3] is taken to vary according to a Gaussian distribution about the mean value $\langle E_J \rangle = \langle I_{J0} \rangle \Phi_0 / 2\pi$, where $\langle I_{J0} \rangle$ is the average maximum Josephson current at zero field. A portion of the equivalent circuit for this system is shown in Fig. 1. This circuit consists of two concentric levels of intragranular regions of area S_0 enclosing an inner normal region of area S_h. One can consider the physical grains to be placed at each node of the network, so that each pair of nodes is separated by a JJ, whose phase difference is denoted by $\varphi_{k,j}$, with k ranging from 1 to 5 and j ranging from 1 to N. If we neglect the mutual inductance coefficients among the elementary current

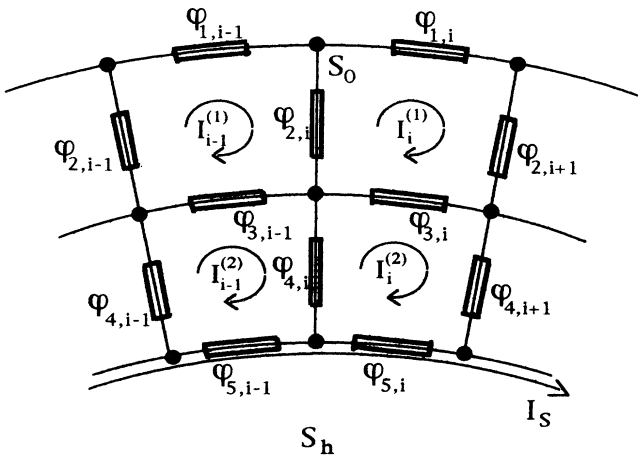

FIG. 1. A portion of the equivalent circuit of a granular system consisting of three concentric granular shells, each shell containing N grains. The rectangles are JJ's: The corresponding phase differences are denoted by the quantity $\varphi_{k,i}$. The currents $I_i^{(j)}$ circulating around the elementary loops of area S_0 are shown along with the current I_S circulating around the inner normal region of area S_h.

loops, we may write the following current-flux equations:

$$\Phi_i^{(j)} = L_0 I_i^{(j)} + \mu_0 H S_0, \quad j=1,2, \; i=1,N$$
$$\Phi_s = z L_0 I_s + \mu_0 H S_h \; , \tag{3}$$

where the index j represents the intergranular level considered and the index i represents the angular position of the elementary loop of area S_0. Therefore, $\Phi_i^{(j)}$ is the flux linked to the ith loop in the jth intragranular level and $I_i^{(j)}$ is the corresponding loop current, while Φ_s is the flux linked to the inner hole of area S_h and I_S is the corresponding loop current. We take $z = S_h / S_0$.

Since fluxoid quantization is a necessary condition for having a single valued superconducting wave function, it must hold for any closed loop interrupted by an arbitrary number of JJ's. Therefore, referring to Fig. 1, we get the following flux-phase relations:

(i) external loops,

$$\varphi_{1,i} + \varphi_{2,(i+1) \bmod N} - \varphi_{3,i} - \varphi_{2,i} + 2\pi \Phi_i^{(1)} / \Phi_i = 0, \quad i=1,N \tag{4a}$$

(ii) inner loops,

$$\varphi_{3,i} + \varphi_{4,(i+1) \bmod N} - \varphi_{5,i} - \varphi_{4,i} + 2\pi \Phi_i^{(2)} / \Phi_0 = 0, \quad i=1,N \tag{4b}$$

(iii) inner hole,

$$\sum_{i=1}^{N} \varphi_{5,i} + 2\pi \Phi_S / \Phi_0 = 0 \; . \tag{4c}$$

The right-hand side of the above equations is null because of the ZFC initial conditions [compare to Eq. (2)]. Neglecting capacitive and thermal fluctuations effects, we can write the dynamic equations for the gauge-invariant phase differences $\varphi_{k,i}$ of the junctions by means of the resistively shunted junction (RSJ) model:[3]

$$\left[\frac{\Phi_0}{2\pi R_n} \right] \frac{d\varphi_{1,i}}{dt} + \alpha_{1,i}(T) \langle I_{J0} \rangle \sin \varphi_{1,i} = \langle I_{J0} \rangle i_i^{(1)} \; , \tag{5a}$$

$$\left[\frac{\Phi_0}{2\pi R_n} \right] \frac{d\varphi_{2,i}}{dt} + \alpha_{2,i}(T) \langle I_{J0} \rangle \sin \varphi_{2,i} = \langle I_{J0} \rangle (i_{i-1}^{(1)} - i_i^{(1)}) \; , \tag{5b}$$

$$\left[\frac{\Phi_0}{2\pi R_n} \right] \frac{d\varphi_{3,i}}{dt} + \alpha_{3,i}(T) \langle I_{J0} \rangle \sin \varphi_{3,i} = \langle I_{J0} \rangle (i_i^{(2)} - i_i^{(1)}) \; , \tag{5c}$$

$$\left[\frac{\Phi_0}{2\pi R_n} \right] \frac{d\varphi_{4,i}}{dt} + \alpha_{4,i}(T) \langle I_{J0} \rangle \sin \varphi_{4,i} = \langle I_{J0} \rangle (i_{i-1}^{(2)} - i_i^{(2)}) \; , \tag{5d}$$

$$\left[\frac{\Phi_0}{2\pi R_n} \right] \frac{d\varphi_{5,i}}{dt} + \alpha_{5,i}(T) \langle I_{J0} \rangle \sin \varphi_{5,i} = \langle I_{J0} \rangle (i_s - i_i^{(2)}) \; , \tag{5e}$$

where the index i ranges from 1 to N. We remark that in granular superconductors the coupling among the grains results similar to a weak link rather than to a planar tunnel junction, so that it is possible to neglect capacitive effects and analyze the overdamped case only, as in Eqs. (5).

In Eqs. (5) we set $i_i^{(j)}=I_i^{(j)}/\langle I_{J0}\rangle$, $i_s=I_s/\langle I_{J0}\rangle$, and $\alpha_{k,i}(T)=I_{J(k,i)}(T)/\langle I_{J0}\rangle$, where $I_{J(k,i)}(T)$ is the maximum Josephson current (which for simplicity has been taken to be field independent) of the junction labeled with the index pair (k,i). The values of the coefficients $\alpha_{k,j}$ are assumed to have a Gaussian distribution about a unitary mean and to be randomly spread over the network. Finally, the T dependence of the maximum Josephson current $I_{J(k,i)}$ can be assumed to be given by the usual Ambegaokar-Baratoff formula.[4]

B. Numerical results

We solve the dynamic equations of the phase differences [Eqs. (5)], which are coupled through Eqs. (3) and (4), by means of an adaptive multistep Runge-Kutta-Merson algorithm. The steady-state solutions are obtained by letting the system involve to its stationary state for each small increase of the forcing term $\xi_{\rm ext}=\mu_0 HS_0/\Phi_0$. Before integrating Eqs. (5) the following normalized quantities have been defined: $\beta_0=L_0\langle I_{J0}\rangle/\Phi_0$, $\xi_i^{(j)}=\Phi_i^{(j)}/\Phi_0$, and $\Psi_s=\Phi_s/\Phi_0$.

A representation of the process of flux penetration in the external intergranular level at very low fields and temperatures is given in Fig. 2 for $\beta_0=3.0$. It must be noted that, for values of the parameter β_0 sufficiently greater than $1/(2\pi)$, the intergranular elementary loops will trap flux quanta irreversibly.[3] In Fig. 2 two types of stationary states can be detected: cylindrically symmetric stationary (CSS) states and cylindrically asymmetric stationary (CAS) states. In the CSS states the flux quanta are shared symmetrically among the intergranular regions, while in the CAS states, this symmetry is not present. From Fig. 2 we also note that, in order for the system to go from one level of CSS states to a different one, it must pass through several CAS states. This is because we assumed that the JJ's are different among them, so that flux quanta do not penetrate symmetrically. In fact, the weaker junctions in the outer elementary loops will allow flux penetration at lower values of the local-field gradient;[7] i.e., at lower values of the effective current flowing in the branch where these junctions are located.

In Figs. 3(a) and 3(b) we show the average flux and the average current, respectively, for both the first and the second intergranular levels. In Figs. 4 and 5 we show the variance of the fluxes and currents, respectively, for both the first and the second intergranular levels. From this numerical analysis we note that the CSS states, as expected, are characterized by a zero variance value of the fluxes and currents. This means that for this class of states the current flowing in the radially oriented branches of the equivalent network of Fig. 1 are zero, so that the effective current distribution is circularly symmetric. In this way, in experimental situations in which only macroscopic quantities are to be measured, one can neglect CAS states and consider only CSS states. We remark that the obtained results are almost completely in-

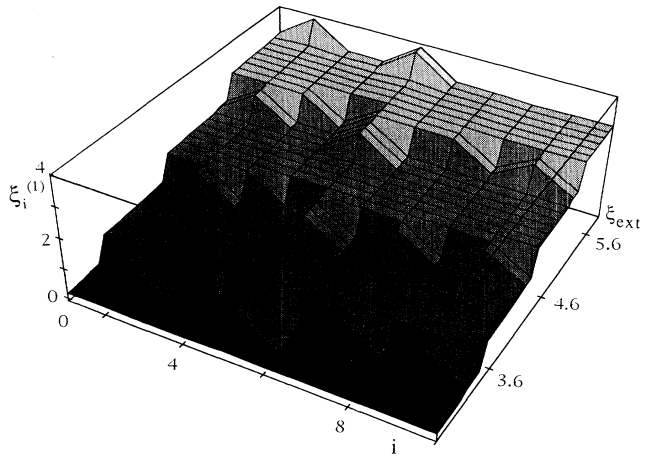

FIG. 2. Representation of the process of flux penetration in the external intergranular level. The i axis represents the angular position of the elementary intergranular loops of the external level. The following choice of parameter has been made: $N=10$, $\beta_0=3.0$, $z=20.0$.

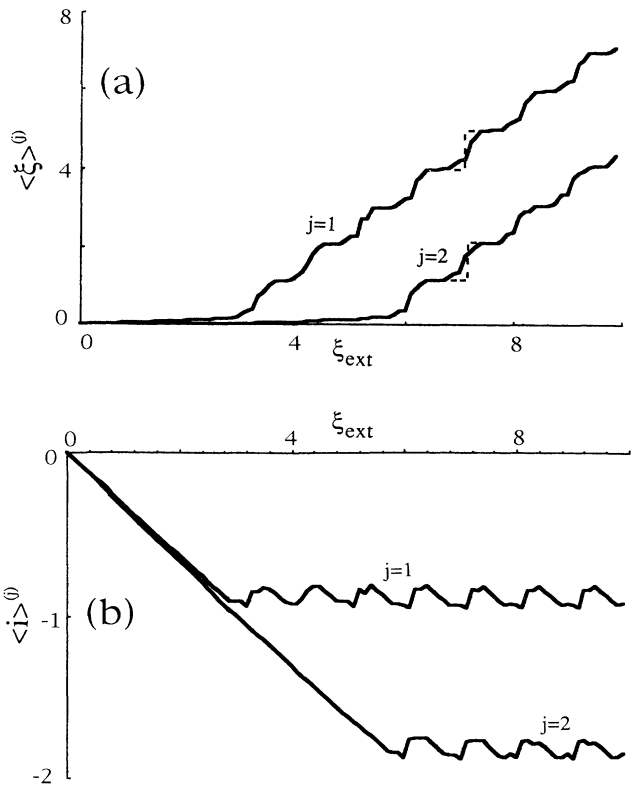

FIG. 3. (a) Average values of the flux trapped in the first ($j=1$) and second ($j=2$) intergranular level of $\xi_{\rm ext}$ ranging from 0 to 10. The dashed portions of the graphs correspond to values of the flux when only CSS states are considered. (b) Average values of the currents trapped in the first ($j=1$) and second ($j=2$) intergranular level for $\xi_{\rm ext}$ ranging from 0 to 10.

dependent of the simplifying assumptions made in the adopted model, since, for values of the parameter β_0 sufficiently greater than $1/(2\pi)$, the process of flux penetration in the first intergranular level does not produce appreciable variations of the phase differences $\varphi_{5,i}$. In this way, the presence of inner intergranular levels is completely irrelevant as far as flux penetration processes in the first intragranular level are concerned.

C. Extension of the model to 3D granular samples

Suppose now we were to consider the macroscopic diamagnetic response of a cylindrical granular sample. We could consider this sample as a stack of identical layers of grains, each layer containing concentric granular shells. When an axial magnetic field is applied, by symmetry considerations, each layer will behave in the exact same way as the rest, so that a bidimensional circuital model can be adopted. Furthermore, by the above discussion, one can simplify the equivalent bidimensional circuit by assuming that only CSS states can be realized in the system. The simplified equivalent network will therefore consist of a set of concentric superconducting rings containing inductively coupled identical Josephson junctions, as shown in Fig. 6.

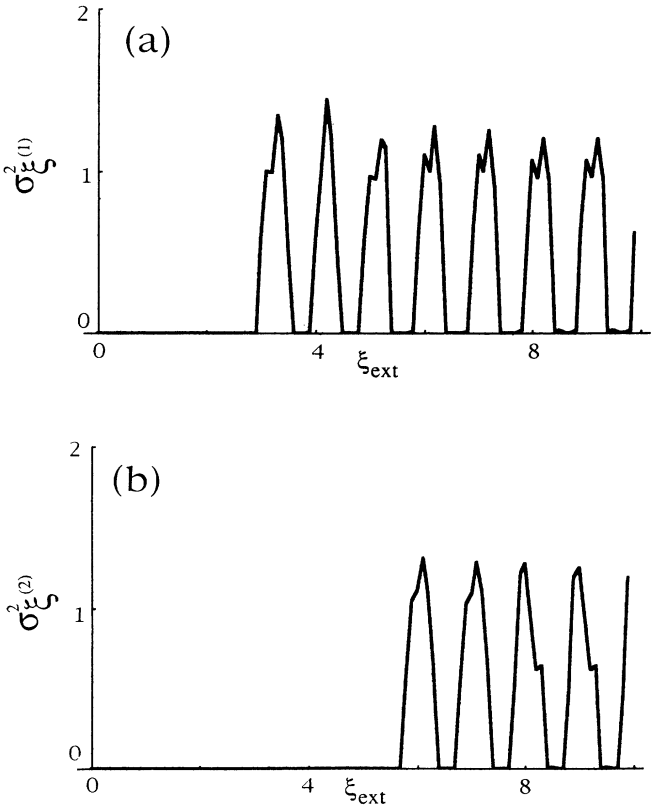

FIG. 4. Variance of the values $\xi_i^{(j)}$ about the average value $\langle \xi \rangle^{(j)}$ for (a) first intergranular level ($j=1$). (b) second intergranular level ($j=2$). The zero variance stationary states represent CSS states.

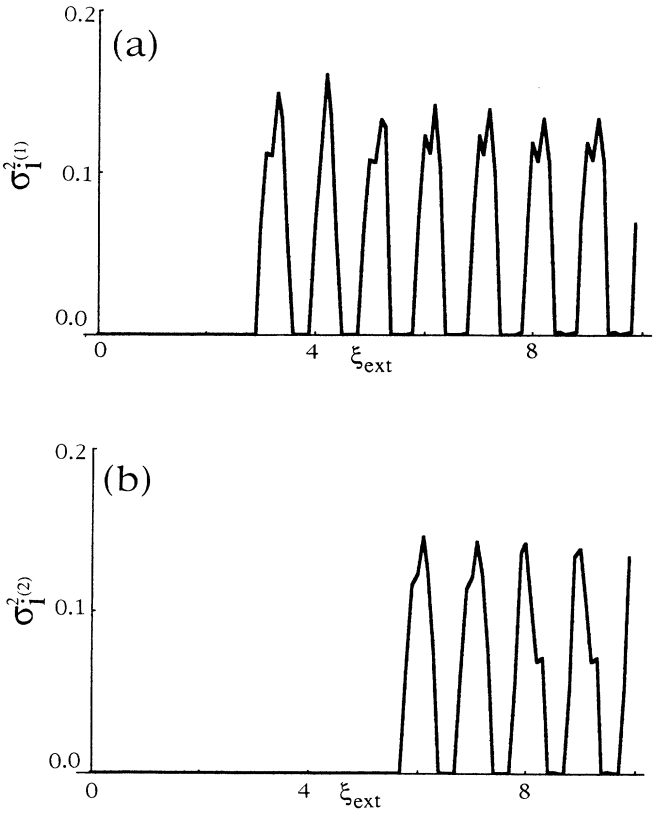

FIG. 5. Variance of the values $I_i^{(j)}$ about the average value $\langle I \rangle^{(j)}$ for (a) first intergranular level ($j=1$). (b) second intergranular level ($j=2$).

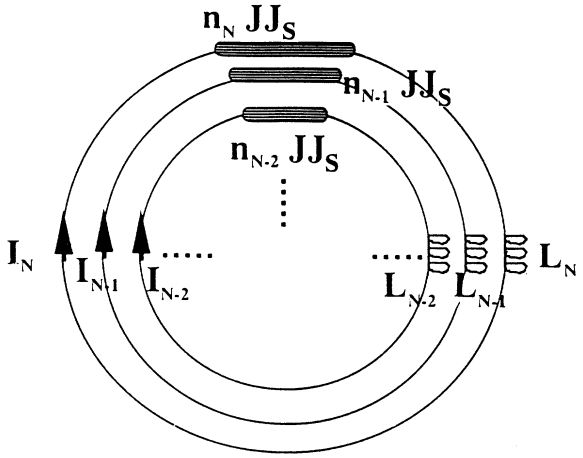

FIG. 6. Concentric superconducting rings containing Josephson junctions. The Josephson junctions in each ring are taken to be proportional to the perimeter of the ring and are all grouped together and represented by shaded sections in the figure.

III. THE SYMMETRIC MODEL

In this section we shall derive the dynamic equations for the system represented in Fig. 6 and derive the experimentally significant quantities from the numerically obtained stationary states.

A. The equations

In Fig. 6 the distance between two adjacent rings is d. The normal area enclosed in the $(N-k)$th ring is written as $S_{N-k}=(N-k)^2S_0$, where $S_0=(\pi d^2)/p$, $1/p$ being the average ratio of the normal area to the total area in the system. The number of junctions n_{N-k} in the $(N-k)$th ring is proportional to the ring perimeter and can be expressed as follows:

$$n_{N-k}=2\pi(N-k)/\eta \ , \tag{6}$$

where $\eta=\Delta s/d$, Δs being the spacing between any two adjacent junctions in the same ring. In what follows we shall take $\eta=\pi$ for simplicity, so that we can write the following simple expressions:

$$S_{N-k}-S_{N-k-1}=n_{N-k}S_0 \ , \tag{7a}$$

$$L_{N-k}-L_{N-k-1}=n_{N-k}L_0 \ , \tag{7b}$$

where L_0 is related to S_0 through the following relation: $L_0=\mu_0 S_0/\lambda$, where λ is some effective length.

The equations for the fluxes Φ_{N-k} linked to the $(N-k)$th ring, $K=0,\ldots,N-1$, are the following:

$$\begin{aligned}
\Phi_N &= L_N I_N + \sum_{j\neq 0} M_{N,N-j} I_{N-j} + \mu_0 H S_N \ , \\
\Phi_{N-1} &= L_{N-1} I_{N-1} \\
&\quad + \sum_{j\neq 1} M_{N-1,N-j} I_{N-j} + \mu_0 H S_{N-1} \ , \\
\Phi_{N-k} &= L_{N-k} I_{N-k} + \sum_{j\neq k} M_{N-k,N-j} I_{N-j} + \mu_0 H S_{N-k} \ ,
\end{aligned} \tag{8}$$

where $M_{N-k,N-j}$ are the mutual inductance coefficients between rings. We assume that the flux lines linked to the rings are perfectly vertical in the region of space near our system, so that the mutual inductance coefficients can be expressed in terms of the self-inductances as follows: $M_{N-k,N-j}=L_{\min\{N-k,N-j\}}$, where the index of the inductance coefficient is the minimum between $(N-k)$ and $(N-j)$. Let us now subtract two successive equations in the set of Eqs. (8), keeping in mind the geometrical quantities related to Eqs. (6) and (7) and defining the following normalized variables:

$$\xi_{\rm ext}=\mu_0 H S_0/\Phi_0, \quad \beta_0=L_0/I_{J0}/\Phi_0, \quad i_{N-k}=I_{N-k}/I_{J0} \ ,$$

$$\xi_{N-k}=(\Phi_{N-k}-\Phi_{N-k-1})/n_{N-k}\Phi_0 \text{ and } \xi_1=\Phi_1/n_1\Phi_0 \ .$$

The quantity ξ_{N-k} represents the number of fluxons localized in the annulus situated between the $(N-k)$th and the $(N-k-1)$th ring normalized to the number of junctions in the $(N-k)$th ring. We thus obtain

$$\begin{aligned}
&\xi_N-\xi_{\rm ext}=\beta_0 i_N \ , \\
&\xi_{N-k}-\xi_{\rm ext}=\beta_0(i_N+i_{N-1}+\cdots+i_{N-k}) \ .
\end{aligned} \tag{9}$$

Equation (6) can now be inverted to obtain the currents i_{N-k} in terms of the variables ξ_{N-k} in the annuli and the externally applied flux $\xi_{\rm ext}$ as follows:

$$\begin{aligned}
&i_N=(\xi_N-\xi_{\rm ext})/\beta_0 \ , \\
&i_{N-1}=(\xi_{N-1}-\xi_N)/\beta_0 \ , \\
&i_{N-k}=(\xi_{N-k}-\xi_{N-k+1})/\beta_0 \ .
\end{aligned} \tag{10}$$

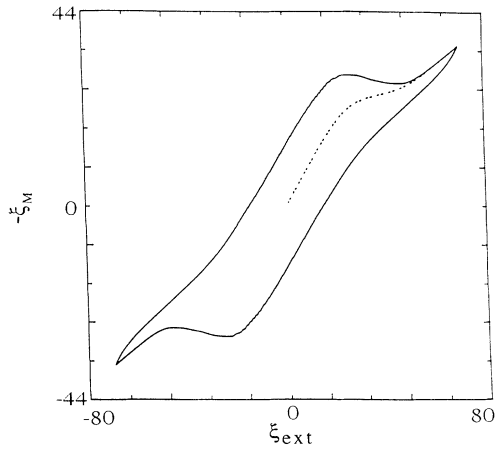

FIG. 7. Negative normalized magnetization ($\xi_M=\mu_0 M S_0/\Phi_0$) vs applied magnetic flux ($\xi_{\rm ext}=\mu_0 H S_0/\Phi_0$) in the range $[-70,70]$ for the concentric superconducting ring system. The following values of the parameters have been used: $\beta_0=5.0$, $N=100$, $a=10.0$, and $p=2.0$. The dashed line corresponds to the first magnetization curve obtained after ZFC.

As in the previous section, neglecting capacitive effects, the dynamic equations for the gauge-invariant phase differences φ_{N-k} of the junctions in the $(N-k)$th ring are written by means of the RSJ model:[3]

$$\begin{aligned}
&(\Phi_0/2\pi R_n)d\varphi_N/dt+\alpha(\xi_{\rm ext},T)I_{J0}\sin\varphi_N=I_{J0}i_N \ , \\
&(\Phi_0/2\pi R_n)d\varphi_{N-k}/dt+\alpha(\xi_{N-k+1},T)I_{J0}\sin\varphi_{N-k} \\
&\qquad\qquad =I_{J0}i_{N-k} \ ,
\end{aligned} \tag{11}$$

where R_n is the resistive parameter of the junction and $\alpha(\xi_{N-k+1},T)=I_{N-k}^{\max}/I_{J0}$, $I_{N-k}^{\max}$ being the local field h and temperature-dependent maximum Josephson current that can flow in the junctions in the $(N-k)$th ring. The coefficients α do not depend on the position indices anymore because of the assumed symmetry and homogeneity of the system. In Eq. (11) we suppose we can neglect stochastic effects due to thermal noise by assuming that the system is immersed in a thermal bath at very low temperatures. For a complete description of the model, one must add the condition of fluxoid quantization to the above equations for any superconducting ring. We notice that under stationary conditions the phase differences across all the junctions in the same ring are equal. Extending this equality to any time t, we may write, under ZFC conditions

$$n_{N-k}\varphi_{N-k}+2\pi\Phi_{N-k}/\Phi_0=0 \ . \tag{12}$$

As for a ring containing a single JJ, Eq. (9) follows directly from the requirement that the superconducting wave function be single valued.[3] The dynamic equations can now be written in terms of the flux variables Φ_{N-k} as follows:

$$(1/n_{N-k}R_n)d\Phi_{N-k}/dt+\alpha(\xi_{N-k+1},T)I_{J0}\sin(2\pi\Phi_{N-k}/n_{N-k}\Phi_0)=-I_{J0}i_{N-k}\ , \tag{13}$$

for $k=0,\ldots,N-1$. By normalizing the time variable as $\tau=R_nt/L_0$, by expressing the ring flux variables Φ_{N-k} in terms of the ξ_{N-k} variables, and by considering Eqs. (10), after subtraction of two consecutive expressions in Eqs. (13), we can finally write the dynamic equations as follows:

(i) for ξ_N,

$$d\xi_N/d\tau+\beta_0[\alpha(\xi_{\rm ext},T)\sin(2\pi\sigma_N/n_N)-\alpha(\xi_N,T)(n_{N-1}/n_N)\sin(2\pi\sigma_{N-1}/n_{N-1})]+(1+n_{N-1}/n_N)\xi_N$$
$$=\xi_{\rm ext}+n_{N-1}\xi_{N-1}/n_N\ , \tag{14a}$$

(ii) for $\xi_{N-k};k=1,\ldots,N-2$,

$$d\xi_{N-k}/d\tau+\beta_0[\alpha(\xi_{N-k+1},T)\sin(2\pi\sigma_{N-k}/n_{N-k})-(n_{N-k-1}/n_{N-k})\alpha(\xi_{N-k},T)\sin(2\pi\sigma_{N-k-1}/n_{N-k-1})]$$
$$+(1+n_{N-k-1}/n_{N-k})\xi_{N-k}=\xi_{N-k+1}+(n_{N-k-1}/n_{N-k})\xi_{N-k-1}\ , \tag{14b}$$

(iii) for ξ_1,

$$d\xi_1/d\tau+\beta_0\alpha(\xi_2,T)\sin(2\pi\xi_1)+\xi_1-\xi_2\ , \tag{14c}$$

where $\sigma_{N-k}=n_{N-k}\xi_{N-k}+n_{N-k-1}\xi_{N-k-1}+\cdots+n_1\xi_1$, for $k=0,\ldots,N-2$.

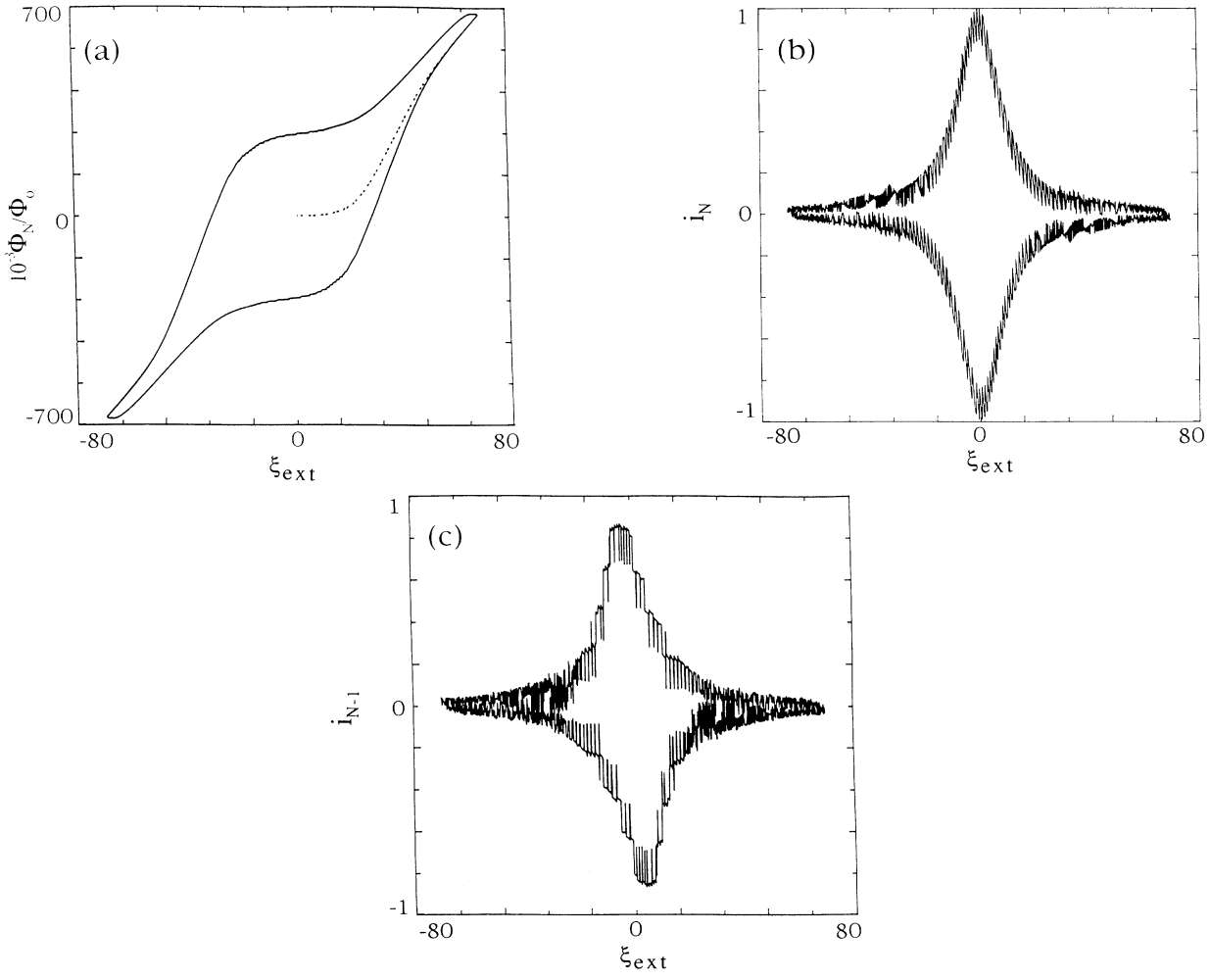

FIG. 8. (a) External field dependence of the total flux number Φ_N/Φ_0 for the same cycle of $\xi_{\rm ext}$ as in Fig. 2. The dashed line corresponds to the first increase of $\xi_{\rm ext}$ after ZFC. The following values of the parameters have been used: $\beta_0=5.0$, $N=100$, $a=10.0$, and $p=2.0$. (b) External field dependence of the current circulating in the outermost (Nth) ring for the same choice of parameters as in (a). (c) External field dependence of the current circulating in the $(N-1)$th ring for the same choice of parameters as in (a) and (b).

B. Numerical results

Analyzing the penetration process of flux quanta in the symmetric model[8] one obviously finds CSS states, which are identical to the CSS states of the asymmetric model. In this way, the symmetric model reduces drastically the number of degrees of freedom of the system, leaving unaltered its macroscopic magnetic characteristics.

Simulations of a magnetization experiment have been performed for temperatures close enough to $T=0$ K, in such a way that thermally activated flux jumps from one annulus to an adjacent one could be neglected. In this temperature limit we can take the function $\alpha(\xi,T)$ to be $\alpha_0(\xi)=\alpha(\xi,T=0)$. We shall analyze finite temperature effects in a future work. An analytic function that fits the functional average of the Fraunhofer patterns arising from the field dependence of $I^{\max}$ for small rectangular junctions is the following:[9,10]

$$\alpha_0(\xi)=a^2/(a^2+\xi^2)\ . \tag{15}$$

In Eq. (15) the characteristic parameter a determines the width of the curve α_0 vs ξ. The set of dynamical Eqs. (14a)–(14c) has been integrated numerically as in Sec. II B. Making use of Eq. (15) in our numerical analysis, we obtained a complete magnetization cycle, the $-\xi_M$ vs $\xi_{\rm ext}$ curve shown in Fig. 7, for $\xi_{\rm ext}$ ranging in the interval $[-70,70]$, and for the following choice of the parameters: $\beta_0=5.0$, $N=100$, $a=10.0$, and $p=2.0$. The normalized magnetization is given by the following expression: $\xi_M=-\xi_{\rm ext}+\Phi_N/(N^2p)$. In Fig. 7 we notice a complete qualitative agreement of the $-\xi_M$ vs $\xi_{\rm ext}$ curve from our model with the experimental magnetization curves of granular high-T_c superconductors (HTS's) reported by many authors.[11,12] In a future work we shall analyze a numerical procedure to obtain the best fit of

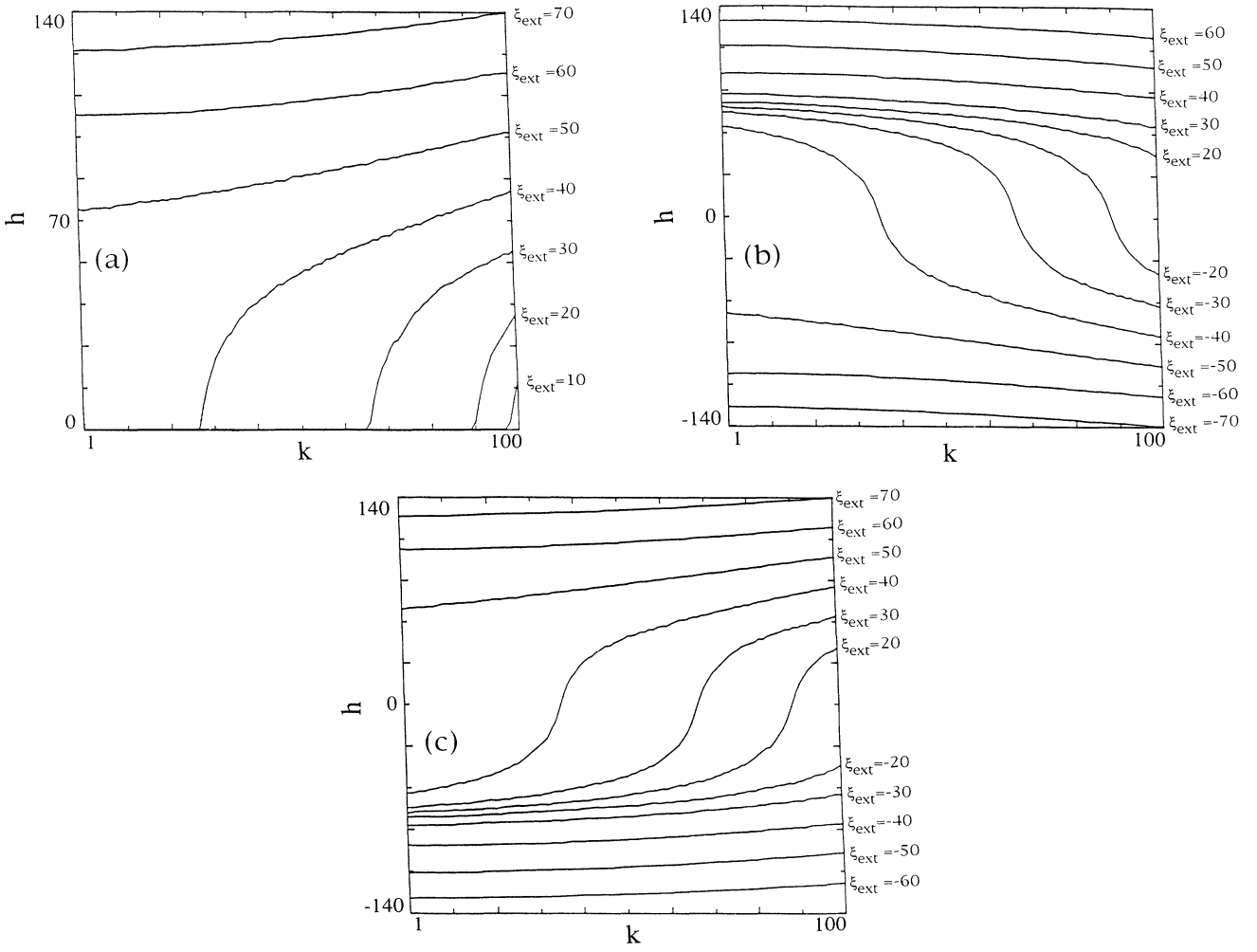

FIG. 9. (a) Distribution of the normalized magnetic flux h in the concentric superconducting rings for increasing values of the applied field, starting from ZFC conditions. (b) Distribution of the normalized magnetic flux h in the concentric superconducting rings for decreasing values of the applied field, starting from $\xi_{\rm ext}=60$ down to $\xi_{\rm ext}=-70$. (c) Distribution of the normalized magnetic flux h in the concentric superconducting rings for increasing values of the applied field, starting from $\xi_{\rm ext}=-60$ up to $\xi_{\rm ext}=70$. The k index represents the radial distance from the center of the system. The values of the parameters are the same as in Figs. 7 and 8.

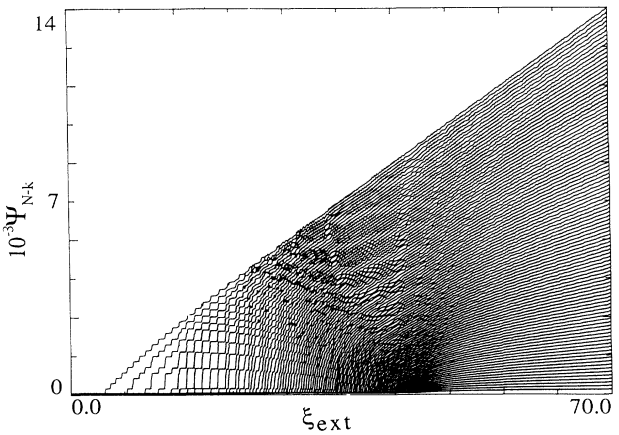

FIG. 10. Representation of the curves of all the flux variables $\Psi_{N-k}=(\Phi_{N-k}-\Phi_{N-k-1})/\Phi_0=n_{N-k}\xi_{N-k}$ for increasing ξ_{ext} values. The variable Ψ_{N-k} represents the total number of flux quanta in the $(N-k)$th shell. The values of the parameters are the same as in Figs. 7, 8, and 9.

these experimental curves by opportunely adjusting the parameters of the model.

The essential features of the numerically obtained magnetization curve are a first almost linear reversible increase with ξ_{ext} up to a threshold normalized field ξ_{gc1} at which first irreversible magnetic-flux penetration takes place. The numerical value of ξ_{gc1} is in agreement with the approximate analytical expression found in Ref. 13:

$$\xi_{gc1}=\{i_c\beta_1+\gamma[1/4+(1/2\pi)\sin^{-1}(1/2\pi\beta_1)]\}\ , \quad (16)$$

where $i_c=[1-(1/2\pi\beta_1)^2]^{1/2}$ and $\gamma=(1+2\pi\beta_1)/2\pi\beta_1$, with $\beta_1=\beta_0\alpha_0(\xi_{ext})$. A negative curvature is present for fields greater than ξ_{gc1} and up to an inflection point corresponding to irreversible penetration of the magnetic field in the last annulus, i.e., corresponding to full penetration. For higher values of ξ_{ext} the curve approaches the asymptote $-\xi_M=(1-1/p)\xi_{ext}$, corresponding to the shielding of only the superconducting portion of the concentric ring system.

In Fig. 8(a) the normalized total flux is shown. In Fig. 8(b) and in Fig. 8(c) the currents in the Nth and in the $(N-1)$th ring, respectively, are shown for the same value of the parameters and for the same cylindrical variation of ξ_{ext}. The hysteretic character of the corresponding experimental curves for HTS's has been also reported in the literature.[14] Furthermore, we give a representation of the field distribution inside the system by fixing the normalized external field ξ_{ext} and by plotting the values of ξ_{N-k} vs increasing k indices. These distributions are shown for ξ_{ext} increasing from 0 to 70 in Fig. 9(a), for ξ_{ext} going from 60 to -70 in Fig. 9(b), and for ξ_{ext} increasing again from -60 to 70 in Fig. 9(c). In Fig. 10 we finally show the curves of the total flux quanta contained in each annulus in terms of the normalized external field ξ_{ext}.

IV. CONCLUSION

We proved that a system of concentric superconducting rings interrupted by inductively coupled identical JJ's can be adopted to describe the low-field diamagnetic response of superconducting granular systems. We derived the dynamic equations for this model, in which the number of junctions in each ring was taken to be proportional to the perimeter of the ring itself. The stationary magnetic states of the system were determined by integrating the set of first-order nonlinear coupled ordinary differential equations found in terms of the magnetic flux.

The irreversible character of flux penetration in the concentric rings gives rise to hysteresis in the system's magnetic quantities. Indeed, the resulting magnetization curves are quite similar to those found in high-T_c granular superconductors. We therefore believe that this simple model, among the various JJ-array models reported in the literature,[4-6,15] can also be adopted to describe the low-field diamagnetic response of this class of superconductors. In a future work we shall give a procedure to optimize the parameters of the model for a given experimental output relative to high-T_c granular superconductors in order to establish a closer link between the model and these physical systems. In this coming work we shall also discuss magnetic relaxation phenomena at finite temperatures by adding stochastic terms,[3] related to flux fluctuations in the superconducting loops of the network, in the dynamic equations of the junctions.

[1]J. Kurkijarvi, Phys. Rev. B **6**, 832 (1972).
[2]H. J. T. Smith and J. A. Blackburn, Phys. Rev. B **12**, 940 (1975).
[3]A. Barone and G. Paternò, *Physics and Application of the Josephson Effect* (Wiley, New York, 1982).
[4]J. R. Clem, Physica C **153-155**, 50 (1988).
[5]A. Majhofer, T. Wolf, and W. Dieterich, Phys. Rev. B **44**, 9634 (1991).
[6]D. Dominguez and J. V. José, Phys. Rev. Lett. **69**, 514 (1992).
[7]R. De Luca, S. Pace, and B. Savo, Phys. Lett. A **154**, 185 (1988).
[8]R. De Luca, S. Pace, and G. Raiconi, Phys. Lett. A **172**, 391 (1993).
[9]S. L. Ginzburg, V. P. Khavronin, G. Yu. Logvinova, I. D. Luzyanin, J. Herrmann, B. Lippold, H. Borner, and H. Schmiedel, Physica C **174**, 109 (1991).
[10]G. Paternò, C. Alvani, S. Casadio, U. Gambardella, and L. Maritato, Appl. Phys. Lett. **53**, 609 (1988).
[11]V. Calzona, M. R. Cimberle, C. Federghini, M. Putti, and A. S. Siri, Physica C **157**, 425 (1989).
[12]K.-H. Muller, J. C. MacFarlane, and R. Driver, Physica C **158**, 69 (1989).
[13]S. Pace and R. De Luca, Physica C **180**, 176 (1991).
[14]V. Ottoboni, A. M. Ricca, G. Ripamonti, and S. Zannella, IEEE Trans. Magn. **24**, 1153 (1988).
[15]D. Stroud and C. Ebner, Physica C **153-155**, 63 (1988).